

Machine Learning Approaches to Bark Beetle Infestation Detection in Alpine Forests

Research Paper for the Marshall Plan Foundation

By

Chandler Ross
Department of Geography
San Diego State University

Supervisor Home Institution:

Dr. Douglas Stow
Department of Geography
San Diego State University

Supervisor Host Institution:

Dr. Gernot Paulus
Department of Geoinformation and Environmental Technologies
Carinthia University of Applied Science

Abstract

Spruce bark beetles (*Ips typographus*), which have been a normal part of the ecosystem, have become a problem for the Austrian Alps in recent year due to warmer temperatures. They attack Norway Spruce (*Picea abies*) in greater numbers than in previous years, which kills the trees and creates a greater chance for avalanches and landslides. This threatens human settlements in the area. Early detection of bark beetles during their early “green stage attack” from May to July gives managers enough time to treat and save the trees. I compared spectral thresholding and a random forest machine learning model to detect the bark beetles using Sentinel-2 data with Planet Labs Planetscope data as reference. I was not able to create an accurate model for detection, but future research should focus on improved training data, random forest parameter selection, and more advanced models such as a convolution neural net.

Acknowledgments

I would like to thank everyone who was involved in this project starting with my advisors both at my home university of San Diego State University and my host university of Carinthia University of Applied Sciences, Dr. Doug Stow and Dr. Gernot Paulus. Thank you for putting in the time and knowledge for assisting me with this project. They both worked hard to schedule a time that worked for both California and Austria. Dr. Paulus was incredibly helpful by checking in on the progress and always offering support.

I would also like to express gratitude to the people at the Carinthia University of Applied Science who helped me transition to working at the school. Though many administrators helped me make the school feel like home, I want to especially thank Alex Maurer, who was a huge help at getting me situated and working.

I would also like to thank the people at the Avalanche and Torrent Control Agency. Their support by providing bark beetle infestation location data and by taking time to show us the infestations in person was crucial in creating accurate training data.

Finally, I would like to thank the Austrian Marshall plan Foundation for supporting this research opportunity. I am grateful to have had this amazing opportunity to conduct research for a summer in Austria and am fully appreciative of all the work the foundation is doing to help facilitate Austrian and U.S research collaborations.

TABLE OF CONTENTS

Abstract	1
Acknowledgments	2
Introduction	6
Literature Review	6
Spectral Vegetation Index Thresholding	6
Non-parametric Models	7
Alternative Methods	8
Methods for Bark Beetle Detection	9
Methods	12
Study Site	12
Data Used	12
Implementation	15
Results	17
Discussion	22
Conclusion	25
Future Work	26
References	27

LIST OF TABLES

Table 1: Sentinel-2 Band Descriptions	14
Table 2: Vegetation indices used in the random forest model.....	17
Table 3: Accuracies of the random forest models.	20
Table 4: Validation error matrix for the early May Sentinel-2 data with all of the spectral vegetation indices as inputs.	20
Table 5: Validation error matrix for the late May Sentinel-2 data with all of the spectral vegetation indices as inputs.	21
Table 6: Validation error matrix for the early May Sentinel-2 data with the spectral vegetation indices that showed some separation during the early stage infection window as inputs.	21
Table 7: Validation error matrix for the late May Sentinel-2 data with the spectral vegetation indices that showed some separation during the early stage infection window as inputs.	22

LIST OF FIGURES

Figure 1: Location of the study site in northwestern Carinthia.	13
Figure 2: The spectral response plot for the CCCI spectral vegetation index for healthy (blue) and diseased (orange) trees. The trees are believed to have become infected in 2020. This plot highlights the difficulty of separating healthy from unhealthy trees. The boxes are when early stage infection detection should take place. The red box is when the infection is believed to have occurred.....	18
Figure 3: The spectral response plot for the NDMI spectral vegetation index for healthy (blue) and diseased (orange) trees. The trees are believed to have become infected in 2020. This plot highlights the difficulty of separating healthy from unhealthy trees. The boxes are when early stage infection detection should take place. The red box is when the infection is believed to have occurred.....	19
Figure 4: Pictures from the ground of tree mortality on July 14th, 2022 (photo credit Chandler Ross).	23
Figure 5: The left image shows a Planetscope true color image of the study site on June 15th, 2021. The right image is a Planetscope true color image of the study site on June 4th, 2022. The boxes in the upper right correspond to the images in Figure 4.	24
Figure 6: The left image shows a Planetscope NDVI image of the study site on June 15th, 2021. The right image is a Planetscope NDVI image of the study site on June 4th, 2022. The boxes in the upper right correspond to the images in Figure 4.	24
Figure 7: The image on the left is a masked Sentinel-2 composite image from May 1st to May 15th. The image on the right is a classified image from a random forest model. Green is healthy trees, red is predicted infected trees, black is shadow, yellow is bare ground, grey is snow, and brown is dead trees. The boxes in the upper right correspond to the images in Figure 4.....	25

Introduction

Spruce bark beetles (*Ips typographus*) have been an increasing problem for Austrian forests. Years ago, they lived in the ecosystem and damaged an ecologically acceptable amount of trees, but with warming temperatures, they have been thriving and killing many more trees (Wermelinger, 2004). Along with climate change, extreme weather events cause increases in spruce bark beetle attacks (Wermelinger, 2004). The spruce bark beetles specifically target the Norway Spruce (*Picea abies*). Spruce bark beetles start to attack the Norway Spruce from May to July (Huo et al., 2021). This is considered early 'green stage attack' where mitigation is still possible. August to October is middle to late stage infection where the tree can no longer be saved. The trees will be green for one to two years before turning grey. This pest lives across central Europe and poses a problem to many of the forests there (Wermelinger, 1999).

The Norway Spruce are vital to the people and ecosystem in the Alps. Besides providing habitat for wildlife, they protect the towns from landslides and avalanches. With increasing bark beetle attacks, some settlements, such as Mörttschach, will be in danger and may be forced to relocate to a safer location.

In this study, I set out to determine if freely available Sentinel-2 imagery can be used to determine early stage bark beetle infestation. My research questions are: (1) Is Sentinel-2 imagery capable of early stage bark beetle infestation detection? (2) Which method is optimal for early stage bark beetle infestation? In order to answer these questions, I use Sentinel-2 imagery as inputs to compare spectral thresholding to a random forest machine learning model to detect early stage bark beetle infestation.

Literature Review

Spectral Vegetation Index Thresholding

Spectral Vegetation Index thresholding is a simple yet powerful tool for helping the analyst determine what is on the ground. Certain phenomena of interest have a spectral vegetation index value above or below a certain threshold, so by setting the specified threshold, the phenomena reveal themselves. Unfortunately, those thresholds change depending on the ecosystem, thus making global products hard to produce (Laboda et al., 2007). Therefore, a threshold for a specific index and area has to be manually set. Even within a single ecosystem, there can be other effects that can change the threshold (Key, 2006). One of the largest drawbacks of spectral vegetation index thresholding is seasonal changes in the image. These seasonal changes are caused both by the time of year (difference in sun angle which changes the reflectance values on the ground) as well as the phenomena of interest (vegetation changes seasonally). Fortunately, for endeavors such as bark beetle tree mortality detection where the window of detection is a small time of the year, these seasonal changes are less of a concern.

Hazy conditions are still a concern for comparing spectral vegetation index thresholds of different years, so it is important to obtain cloud free data.

Non-parametric Models

Machine Learning (ML) is a powerful method for classifying imagery quickly. Several methods exist including gradient boosted regression models (GBRM), random forests (RF), artificial neural networks (ANN), support vector machines (SVM), and classification & regression trees (CART), among others (Jensen, 2015). A possible drawback to ML is it requires accurate and abundant training data in order to work effectively.

Artificial neural network classifiers are powerful at classifying features and have been used in remote sensing applications (Jensen, 2015; Qiu and Jensen, 2004). This method does not make assumptions about the data and can use object based image analysis (OBIA), pixel, and/or ancillary data (Jensen, 2015; Qiu and Jensen, 2004). ANNs contain an input layer, hidden layer(s), and an output layer. The ANN learns through backpropagation and weights are applied to different connectors in the neuron. One downside to an ANN is there is a “black box” element to it; it is hard to know exactly why it works in a given circumstance. Qui and Jensen (2004) set out to try and “illuminate” some of the mysteries of the black box by merging it with a fuzzy expert system to make the decision rules clearer.

Classification and decision trees are a very simple ML method. They work by running variables through various sets of decision trees to determine classes. CART is older and less robust compared to other ML algorithms, but it does serve as a basis for more powerful algorithms like RF and GBRM (Hawbaker et al., 2017). Support vector machines are another useful classification method that transforms the data into higher and higher dimensions until a hyperplane can separate the data (Jensen, 2015). A benefit is they do not need a large training set and have been found to have similar results as an RF (Pal and Mather, 2005).

Random Forests have been found to be a robust method for remotely sensed image classification (Collins et al., 2018). RFs work by creating many classification decision trees and the data is processed through decision trees with random variables at each node and each tree votes on how the pixel should be classified. The most votes determine the classification (Jensen, 2015). Unlike SVM which works well with few data, RF needs a lot of data to work well, which is a good application for remote sensing since it inherently has a lot of data. Collins et al. (2018) found RF to be better than individual spectral indices when classifying satellite imagery in Australia.

Gradient boosting regression models are similar to a CART in that its basis is a CART model where each observation is used to better fit the model depending on how big a residual is from the previous CART model. The bigger the residual, the smaller the weight is of the output. The GBRM model is more accurate than a regular CART and even a random forest when it comes to binary decisions, plus it has extensive use in remote sensing applications (Hawbaker et al., 2017). The algorithm does not assume independence among its predictors and can handle correlated predictors (Hawbaker et al., 2020). However, more variables, especially correlated

ones, may not improve the accuracy (Hawbaker et al., 2020). Hawbaker et al. (2020) model wanted to reduce computation time from useless predictors so they selected the variables that would not correlate as much.

Alternative Methods

There are several methods for detecting a change in a time series of remotely sensed images. Some of the popular ones that have been used for detecting bark beetle infestations are Continuous Change Detection and Classification (CCDC) and Landsat-based detection of Trends in Disturbance and Recovery (LandTrendr). Others have been used for change detection, but have not been applied specifically to bark beetle infestation detection such as Breaks For Additive Season and Trend (BFAST) and Bayesian Estimator of Abrupt change, Seasonal change, and Trend (BEAST).

Continuous Change Detection and Classification is a useful method for detecting change using a time series, at any point in the time series (Zhu et al., 2012; Zhu & Woodcock, 2014). This is useful for detecting recent changes. The algorithm works by first removing noise, such as clouds, then uses a threshold derived from all the input bands to detect change (Zhu & Woodcock, 2014). When the pixel exceeds the threshold three consecutive times, a change is registered. Studies utilizing continuous change detection have been used for detecting bark beetle infection (Grabska et al., 2020). The algorithm proved useful in determining bark beetle infestation. However, this algorithm has been used more often to monitor past change rather than current change. Other researchers have used their own algorithms that are based on similar designs to detect bark beetles, and have found success (Ye et al., 2021). The upside is theoretically, this algorithm, and those like it, can quickly detect change in a forest. The downside is in order to reduce the chances of false positives, three passes are needed. So for Sentinel-2 data, it would take 15 days minimum from when the change started to when it could be detected. If Landsat is used, or if there are clouds, the minimum amount of time would be increased.

Landsat-based detection of Trends in Disturbance and Recovery is as the name implies a Landsat approach to detecting trends, and specifically disturbances, in a time series of data for the same area. The algorithm takes a time series of images and applies a temporal segmentation on it using a band or a spectral vegetation index. This creates a model where change can be detected. Each temporal segmentation has a start, end, duration, magnitude, and speed of change. (Kennedy et al., 2010). The algorithm recognizes that change is not just a difference between two points in time but rather a continual process. LandTrendr has been found to be useful for detecting bark beetle infested areas (Bright et al., 2014; Senf et al., 2015). However, it has mostly been used for long term trends and late stage detection of bark beetles. Though it can be used to distinguish bark beetle attacks from other types of disturbances, it has not been widely used for early stage bark beetle detection (Senf et al., 2015). It is useful since it accesses the Landsat archive, which has useful data going back to 1984, but it has a 30 m ground sample

resolution which is wide for detecting early stage infection. Lastly, the algorithm is easy to implement with Google Earth Engine and ESRI products.

The Breaks for Additive Season and Trend algorithm and Bayesian estimator of abrupt change, seasonal change, and trend algorithms have shown promise in forest change detection, but have yet to be applied to bark beetle infestation detection. The BFAST family of change detectors (BFAST, BFAST monitor, and BFAST lite) detect the change by decomposing a time series into trend, seasonal, and remainder components, and uses that to determine the change from seasonal trends (Masiliūnas et al., 2021; Verbesselt et al., 2010). The changes are characterized by change and direction. This provides another tool for detecting bark beetle infestations, and separates seasonal change from unexplained change. The BEAST algorithm is an ensemble that works by quantifying the relative usefulness of other decomposition models (Zhao et al., 2019). Ensemble models can be powerful because they bring together other models to yield a more accurate result. This has been used in many remote sensing applications for forest change detection (Giannetti et al., 2021; Hu et al., 2021). The algorithm has been used with programs such as Google Earth Engine, which makes it easy to implement to other areas. There are many different algorithms for change detection, but these could prove to be useful ones for early stage bark beetle detection.

Methods for Bark Beetle Detection

Traditional methods of determining if a tree is infected with bark beetles involves physically going to trees and manually checking for signs of the beetle. Though this method is considered the most robust for determining infection, it is very time consuming and can let a single person reach a small number of trees in a given period of time. That is why remote sensing is crucial to determining bark beetle infestations. Much more area will be able to be reached in a given amount of time. There are many different methods of remote sensing, each with their own benefits and drawbacks. Unpiloted aerial vehicles (UAV), also known as “drones,” are a common method used for smaller areas. Though the sensors vary, they usually are able to detect a smaller ground sample resolution, or “pixel size,” often from 5 cm to 2 m. The drawback is they cover a smaller area than other remote sensing platforms. They also come with a cost, though UAVs and the subsequent equipment are not unobtainable priced. Aerial imagery generally provides a greater swath width than UAVs, but usually at a smaller ground sample resolution, often from 50 cm to 10 m. Also, they can be expensive to operate, especially for continuous monitoring. Lastly, satellites are often used. Moderate ground sample resolution imagery from governments tend to be freely available with a long backlog of data for the same area, but at a much lower ground sample resolution from 10 m to 30 m depending on the band and satellite used. Along with having a long backlog of data, government satellite data often has a high frequency interval of five to seven days, depending on the satellite constellation. Two governmental satellites often used for bark beetle detection are the Landsat constellation and the Sentinel-2 constellation. Useful Landsat data dates back from 1984 to the present across five different satellites. The return interval per satellite is 14 to 16 days, but with multiple satellites often operating at the

same time, it is more often around seven days. The ground sample resolution is 30 m for the optical and 60 to 90 for the thermal band. Sentinel-2 is a constellation of two satellites that launched in 2015. Its data is 10 m for the visible light and near infrared bands, 20 m for the red edge and shortwave infrared bands, and 60 m for the water vapor bands. Each satellite returns over a given area every 10 days, with a five day return interval between the two satellites. Both Landsat and Sentinel-2 data comes preprocessed for atmospheric correction and ground alignment. Private satellites can provide much higher spatial resolution as well as temporal resolution than government satellites. For example, Planet data covers the same area every day and is 7 m to sub-meter data. However, this data is rarely free and can be quite expensive. They also do not have as long as a data archive as some of the government satellites.

Unpiloted aerial vehicles can be variable in terms of the sensors, so it can be difficult to directly compare studies since different sensors are usually used. However, this allows researchers to compare different techniques to remote sensing. Klouček, (et al., 2019) used a cost effective optical camera using the visible bands red, green, and blue plus the near infrared to monitor *Ips typographus* disturbances in Spruce forests. They were able to find changes in the infected trees, but not before August, which is when it is still possible to mitigate the spread of bark beetles (Klouček et al., 2019). In another study, Lausch (et al., 2013), used a hyperspectral camera with ground sample resolutions at 4 m and 7 m to determine early stage infection. They found that the 4 m was more robust than the 7 m, but the most accurate they were was 64%, which is better than a coin toss but is “insufficient in forestry practices” (Lausch et al., 2013). Though the lower spatial resolution was more robust, it was not found to be obsolete.

Governmental satellites have lower spatial resolutions than UAV mounted sensors, but they generally have increased temporal passes which can help increase the chances of early stage infection detection. Ye (et al., 2021) used Landsat for continuous monitoring of forests in Colorado, USA for mountain pine and spruce disturbances. Their algorithm had an F1 score of 0.73 with a 30 m ground sample resolution for spruce trees infected for two years (Ye et al., 2021). This study scores the difficulty in detecting bark beetle attacks with a greater ground sample resolution. Bright (et al., 2015) used Landsat and lidar data as inputs to a random forest model, and had “low to moderate” spearman correlations, meaning their model was not incredibly accurate at detecting defoliation, underscoring the difficulty of larger ground sample resolution (Bright et al., 2014). Grabska (et al., 2020) used Sentinel-2 to map disturbances in Scott’s Pine and was 75% accurate in doing so using spectral trajectories (Grabska et al., 2020). The higher spatial resolution of 10 m to 20 m with the spectral trajectories is about as accurate as previous studies using 30 m Landsat and machine learning. This shows how a less computational approach can be as accurate as long as a lower resolution is used. Fernandez-Carillo (et al., 2020) used a change detection approach with Sentinel-2 data and achieved above 80% accuracy for late stage infections but was lower for early stage infections. They masked out areas that were not trees and clear cuts which helped focus on areas that mattered. Some researchers used a combination of sensors. Bright (et al., 2015) used Landsat and lidar. The Landsat was better at determining dead trees whereas the lidar was better at determining the healthy ones. The data

helped balance each other. Huo (et al., 2021) used Sentinel-2 optical and Sentinel-1 Synthetic Aperture Radar (SAR) data to detect green stage bark beetle infestations in Norway Spruce. The different data was inputted into a random forest model. They determined that very little detection could be done during the green stage, but that after a storm event, many trees became damaged and that these damaged trees were much more likely to become hosts for the bark beetles. Huo (et al., 2021) looked at stressed trees as a proxy for green stage attack. By detecting the proxy of stress during the months green stage attack happens, they found the red and short wave infrared bands were the most prevalent and achieved an 80% to 88% accuracy. They were able to detect middle and late stage infections with 81% to 91% accuracy. With the low accuracies of the other studies, looking at a proxy, such as tree stress, can be a very important method to determining bark beetle infestation. Another study found that auxiliary data such as a storm event is significant to detecting disturbance (Oeser et al., 2017). Many bark beetles attack after a storm event in Europe so it works for bark beetles as well as general disturbances.

Private satellites have been shown to be robust at detecting bark beetle infestation. Ortiz (et al., 2013) used RapidEye and TerraSAR-X data along with three models: generalized linear models, maximum entropy, and random forest. The minimum mapping unit was 78.5 m² between the two satellite datasets. Using both satellites, they were able to achieve a green stage classification accuracy of 74% (Ortiz et al., 2013). They found that the maximum entropy model was more accurate than the random forest and general linear models. Immitzer (et al., 2014) used WorldView-2 data with a ground sample resolution of 0.46 m and compared a random forest and a logistic regression model to classify the images as “healthy,” “green stage,” and “dead” (Immitzer & Atzberger, 2014). They found that the random forest model was the most accurate, with an accuracy of 75% for the three classes. Both studies that used private satellites for early green stage infection detection achieved a similar result using wildly different minimum mapping sizes of 78.5 m² and 0.1764 m². However, one study utilized SAR data whereas the other used only optical data. Though a lower spatial resolution can be helpful, it is not needed to make a more accurate model.

Both optical and radar sensors have been used for detecting bark beetle infestations. Though radar has been able to help, it is not as efficient as optical sensors at detecting infestations and does not need to be used (Hollaus & Vreugdenhil, 2019; Huo et al., 2021; Ortiz et al., 2013). In terms of optical sensors, there is a debate about which wavelengths are more sensitive to bark beetles for green stage infestation detection. The Huo (et al., 2021) study found that the red and short wave infrared 1 wavelengths are optimal for detecting green stage infestation. Grabska (et al., 2020) also agree that the short wave infrared 1 wavelength is optimal for detection. However, the Lausch (et al., 2013) study found that visible to near infrared (450 nm to 890 nm) was optimal, whereas short wave infrared 1 (1400 nm to 1800 nm) was inefficient. The Ye (et al., 2021) study found spectral vegetation Indices tuned to wetness to be the most useful in early stage detection, which include the near infrared, shortwave infrared 1 & 2, and various Kaut-Thomas transformations. Other studies found the K-T transformations to be prominent predictors (Senf et al., 2015). It should be noted the first three studies used Sentinel-2

whereas the last one used Landsat. There are slight differences in the spectral windows for the bands between the two constellations. Different studies, either with the same sensors or different sensors, have found different wavelengths to be optimal for green stage infection, so there is not a consensus yet on which is the best (Huo et al., 2021).

Methods

Study Site

The study site is located in northwestern Carinthia, Austria's southernmost state, and is 5,427.29 hectares in area (Figure 1). The local avalanche and torrent control district provided polygons where known bark beetle attacks occurred, and a subset of the polygons was used around the town of Mörttschach. These polygons were drawn and it provided a rough outline of where some of the infections were, but the outlines were not perfect. This subset was chosen for ease of processing and a field visit occurred here. It is near where the avalanche and torrent control District office is located, so they are more familiar with the area. The vegetation of the site is composed of Norway Spruce trees, grasses, and some forbs. The terrain of the site is very extreme with a valley in the center and steep mountains on either side. The steep terrain makes the area prone to avalanches. The steep terrain also creates issues for remote sensing due to distortions in the imagery as well as creating shadows. The elevation ranges from 909 m to 2,589 m above sea level. The maximum slope is 75.25 degrees computed from 30 m SRTM data (Farr et al., 2007). Vegetation can be seen without snow from late March to early May, depending on the year, until Winter.

Data Used

Multispectral imagery captured by Sentinel-2A and Sentinel-2B was used to map the location and distribution of Norway Spruce infected by bark beetles for the study area and study period. Sentinel-2A data dates back to 2015 and Sentinel-2B data dates back to 2017. I used level 2A data, which is the highest level of corrected imagery that provides the bottom of atmosphere correction. The reflectance imagery is derived from the level 1C data products and it removes the top of atmosphere cloud haze. The data was retrieved from Google Earth Engine, so the data available on the platform was from 28-03-2017 to the present. The ground sample resolution is 10 m to 60 m depending on the spectral band used. There are 13 different spectral bands ranging from 443.9 nm to 2202.4nm with minimal differences between Sentinel-2A and Sentinel-2B sensors for each band. The band descriptions can be found in Table 1. The temporal resolution is a 10 day repeat pass time for each satellite, and 5 days for the combined constellation revisit.

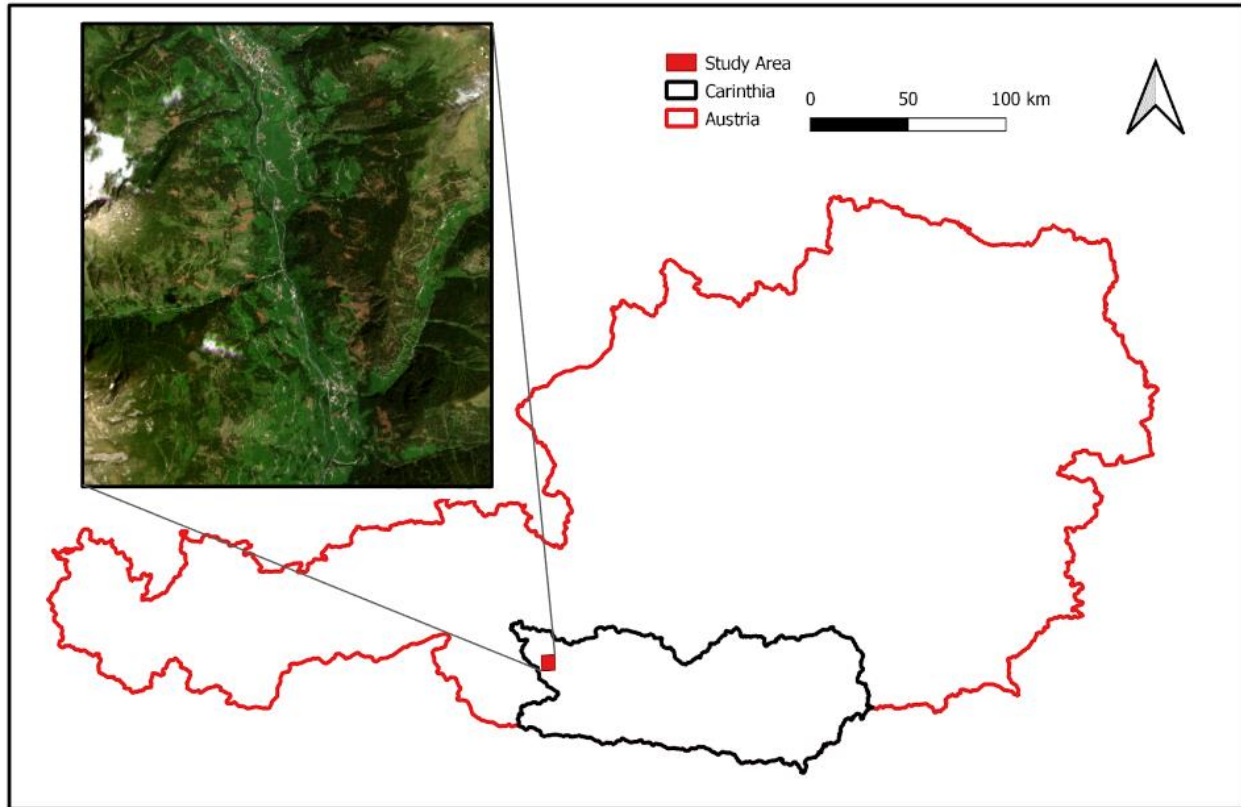


Figure 1: Location of the study site in northwestern Carinthia.

Imagery from Planet Labs was used as reference data for the random forest and thresholding processes. I used Planetscope data which ranges from 3 m to 7 m depending on the image acquired. There are three generations of Planetscope data with different spectral specifications. The first generation had blue, red, green, and near-infrared bands and was launched in June of 2016. The second generation imagery was available in March of 2019 and has the same spectral bands, but an improved method of collection. The third generation imagery availability started in March of 2020 and has eight spectral bands of coastal blue, blue, green 1, green, red, yellow, red edge, and near-infrared. Planetscope data is available daily with a spectral resolution of 12 bits. I downloaded one scene from the months of April and May of 2020, one for each month from April to September of 2021, and one for each month from April to June of 2022. I downloaded these scenes because I wanted to see the spectral change in the Norway Spruce from these time periods and I wanted reference data for each month in the infestation window of April to September. The scenes from 2020 are there to set a baseline for the early stage infestation scenes.

I used vector polygons generated by the local Avalanche and Torrent Control Agency that marked the areas that have been recently attacked by bark beetles. Unfortunately, I did not have metadata on the polygons, so I didn't know when the areas in the polygons were first infected, nor the level of infection within each polygon, nor if the polygons were the only infected areas in the study period, but it was helpful to have confirmed areas of attack. I went

into the area with members from the Avalanche and Torrent Control Agency and my advisors and took pictures of trees infested with bark beetles along with areas not infested. These photos acted as a “ground truth” for infested and noninfested areas, along with the polygons and Planetscope imagery.

Table 1: Sentinel-2 Band Descriptions

Band Name	Wavelength (nm)	Description
1	433 - 453	Coastal Aerosol
2	458 - 552	Blue
3	543 - 557	Green
4	650 - 680	Red
5	698 - 712	Vegetation Red Edge 1
6	733 - 747	Vegetation Red Edge 2
7	773 - 793	Vegetation Red Edge 3
8	785 - 889	Near Infrared
8A	855 - 875	Narrow Near Infrared
9	935 - 955	Water Vapor
10	1360 - 1390	Short Wave Infrared - Cirrus
11	1565 - 1655	Short Wave Infrared 1
12	2100 - 2280	Short Wave Infrared 2

Processing for the project was conducted in Google Earth Engine (GEE). I chose GEE over other image processing software because it has the ability to quickly process large amounts of data both temporally and spatially, with just an internet connection. A computer with quick processing speeds and large storage is not needed. Google Earth Engine also has a large catalog of data which includes the Sentinel-2 level 2A imagery. This saves considerable time not downloading data from the European Space Agency. It is easy to create plots and perform spectral thresholding as well as machine learning with GEE.

Implementation

The goal of this research is to create a tool that is easy to use for the Avalanch and Torrent Control Agency in order to be able to detect early stage infestation of bark beetles in order to curb their spread. With this goal in mind, I tried spectral vegetation index thresholding since that is easy to implement in Google Earth Engine. For spectral vegetation index thresholding, I compared the Disease Water Stress Index (DSWI), Canopy Chlorophyll Content Index (CCCI), Chlorophyll Vegetation Index (CVI), Modified Soil Adjusted Vegetation Index (MSAVI), Normalized Burn Ratio (NBR), Normalized Difference Vegetation Index (NDVI), Normalized Difference Water Index (NDWI), Normalized Difference Moisture Index (NDMI), Ratio Drought Index (RDI), and Red Green Index (RGI) spectral vegetation indices. Each of the spectral vegetation indices are described in Table 2. These were chosen because they have been found to be helpful in bark beetle detection (Huo et al., 2021). I created spectral plots of each of the spectral vegetation indices in Google Earth Engine from April of 2017 to June of 2022. In order to create spectral plots I applied a cloud mask to the Sentinel-2 imagery to remove clouds and cloud shadow. The cloud mask was not perfect, but it removed a great majority of the clouds and cloud shadow. This is important for the spectral plots because clouds and cloud shadow will produce extreme values for the spectral vegetation indices and misrepresent the phenomena on the ground in the plots.

I initially performed an exploratory data analysis with the Sentinel-2 data and the Bark Beetle polygons. In order to do this, I placed 30 points across several polygons and 30 points outside of the polygons. Then I averaged the values and placed them in the plot. After I acquired the high resolution Planetscope data and images from the ground, I found areas with high likelihood of being infected by bark beetles and areas with a high likelihood of having not been infected by bark beetles. I created 60 sample points for the healthy and infected classes and created the spectral plots for each of the spectral vegetation indices for the Sentinel-2 data.

Once the plots were created for the high spatial resolution informed plot-point Sentinel-2 data, I marked where the view window is optimal from April to July. I visually inspected the plots for signs of differences between the infected and noninfected areas. After looking at the initial plots and the high spatial resolution informed plots, I determined that a simple spectral vegetation index thresholding approach was not going to work for the early detection of bark beetles, so I decided to move to a more robust non-parametric method for early stage bark beetle infestation detection.

After the thresholding approach was attempted, I decided to implore a machine learning method, random forests, in order to classify the early stage bark beetle infested trees. I explored classification methods for the early stage infestation of Norway Spruce in the Spring of 2021 since a storm hit the area in the Winter of 2020 - 2021, leaving many damaged trees. Machine learning is able to pick up on many trends that humans cannot recognize on our own. The random forests model is an ensemble approach that can recognize little trends through its tree based majority vote approach, whereas a spectral vegetation index thresholding approach uses less information to achieve the same result. In order to implement the random forest model I

used Google Earth Engine's `smileRandomForest` package. In order to train the data, I compared two different training sets for two different scenes. The first training set used a Sentinel-2 image median composite from May 1st, 2021 to May 15th, 2021. The Planetscope imagery used to inform the training of the Sentinel-2 data was from May 10th, 2021, June 15th, 2021, and June 4th, 2022. The second training set used a Sentinel-2 image median composite from May 20th, 2021 to May 30th, 2021. These dates were chosen to be when the bark beetles attacked. Two were chosen for a comparison of different scene quality. The same Planetscope data was used. For both of the training sets, I compared points and polygons for each of the classes to compare if the slight change in training data would make a difference in classification accuracy. For each of the classes that used points, I ensured that at least 30 points were used. Also, I placed the points a distance away from each other to reduce spatial autocorrelation. I used a class imbalance method where certain classes received more training than other points if they were more prevalent. This is to help ensure that classes with small areas are not overrepresented in the final classification. The classes for the two training sets are similar but slightly different. The first training set from mid-May used the classes of snow, shadow, bare ground, dead trees that remained dead trees a year later, green trees that remained green, and lastly green trees that turned brown a year later. The same classes were used for the second late May training set except for the inclusion of a cloud class. The first image did not have clouds to train on, so the cloud class was omitted. In order to create the training areas for the classes, I looked at areas that appeared to be infected by bark beetles in June of 2022, and compared the areas that didn't appear to be infected by bark beetles in early 2021. Then, I placed the points or polygons in areas over the Sentinel-2 imagery that corresponded to the Planetscope data.

In addition to trying training data for a single image time, I also created training data for the two training sets (mid-May, 2021 and late May, 2021) for differenced spectral vegetation index data. I wanted to see if the addition of a time change would help the prediction of early stage bark beetle infestation classification. To create the training data, I subtracted a composite image from mid-May, 2020 from the mid-May, 2021 composite. The same was done for the late May composites. I used the same training points and polygons for the differenced spectral vegetation index trained approach.

Before running the classification, first I masked the Sentinel-2 data with a cloud mask. The cloud mask was not perfect, but it reduced most of the clouds. Then I applied a mask that ensured only trees were present in the final image. This classification mask was not perfect, but it removed most of the other vegetation classes. This mask was derived from an 11 class land classification product made from 10 m Sentinel-2 data (Zanga et al., 2021). Once I had predominantly tree data, I calculated the spectral vegetation indices of DSWI, CCCI, CVI, MSAVI, NBR, NDVI, NDWI, NDMI, RDI, and RGI whose formulas are listed in Table 2. I also calculated the differenced spectral vegetation indices from the imagery from a year prior. Then I applied the points or polygons for training. Once the training points were set, I inputted all of the spectral vegetation indices. I also compared only using the DSWI, RDI, NDVI, NBR, and NDMI spectral vegetation indices. I chose these because they appeared to have a greater separation in

the spectral charts of the healthy trees and non-healthy trees compared to the ones not used. I used 80% of the training data for training and 20% for validation. For the inputs of the model, I used: 500 trees, 3 variables per tree split, a minimum leaf population of 1, a bag fraction of 0.5, and no limit for the maximum number of nodes. I used these parameters for each of the implementations.

Table 2: Vegetation indices used in the random forest model.

Index	Formula
Disease Water Stress Index (DSWI)	$(Band\ 8 + Band\ 3) / (Band\ 4 + Band\ 11)$
Canopy Chlorophyll Content Index (CCCI)	$((Band\ 8 - Band\ 6) / (Band\ 8 + Band\ 6)) / ((Band\ 8 - Band\ 4) / (Band\ 8 + Band\ 4))$
Chlorophyll Vegetation Index (CVI)	$(Band\ 8A + Band\ 5) / (Band\ 3 * Band\ 3)$
Modified Soil Adjusted Vegetation Index (MSAVI)	$(2 * Band\ 8 + 1 - \sqrt{(2 * Band\ 8 + 1)^2 - 8 * (Band\ 8 - Band\ 4)}) / 2$
Normalized Burn Ratio (NBR)	$(Band\ 8A - Band\ 12) / (Band\ 8A + Band\ 12)$
Normalized Difference Vegetation Index (NDVI)	$(Band\ 8A - Band\ 4) / (Band\ 8A + Band\ 4)$
Normalized Difference Water Index (NDWI)	$(Band\ 3 - Band\ 8A) / (Band\ 3 + Band\ 8A)$
Normalized Difference Moisture Index (NDMI)	$(Band\ 8 - Band\ 11) / (Band\ 8 + Band\ 11)$
Ratio Drought Index (RDI)	$Band\ 12 / Band\ 8A$
Red Green Index (RGI)	$Band\ 4 / Band\ 3$

Results

Neither the thresholding approach nor the random forest approaches were able to detect early stage bark beetle infestation. For the thresholding approaches, I looked for spectral separation for the DSWI, CCCI, CVI, MSAVI, NBR, NDVI, NDWI, NDMI, RDI, and RGI

spectral vegetation indices during the green stage attack time period of mid-April to June. There are no spectral vegetation indices with a clear value to threshold to determine early stage infection. However, five of the spectral vegetation indices showed some change: DSWI, RDI, NDVI, NDMI, and NBR. The others showed no separation at all during the early stage infection period. Figure 2 shows the spectral response plot for healthy and infected trees for the CCCI spectral vegetation index where there is little separation between healthy and unhealthy trees. Figure 3 shows the spectral response plot for healthy and unhealthy trees for NDMI, where there is more separation during the early stage infection window. Though five of the spectral vegetation indices showed a little separation, it was not enough to create an accurate model for early stage infection.

Neither the thresholding approach nor the random forest approaches were able to detect early stage bark beetle infestation. For the thresholding approaches, I looked for spectral separation for the DSWI, CCCI, CVI, MSAVI, NBR, NDVI, NDWI, NDMI, RDI, and RGI spectral vegetation indices during the green stage attack time period of mid-April to June. There are no spectral vegetation indices with a clear value to threshold to determine early stage infection. However, five of the spectral vegetation indices showed some change: DSWI, RDI, NDVI, NDMI, and NBR. The others showed no separation at all during the early stage infection period. Figure 2 shows the spectral response plot for healthy and infected trees for the CCCI spectral vegetation index where there is little separation between healthy and unhealthy trees. Figure 3 shows the spectral response plot for healthy and unhealthy trees for NDMI, where there is more separation during the early stage infection window. Though five of the spectral vegetation indices showed a little separation, it was not enough to create an accurate model for early stage infection.

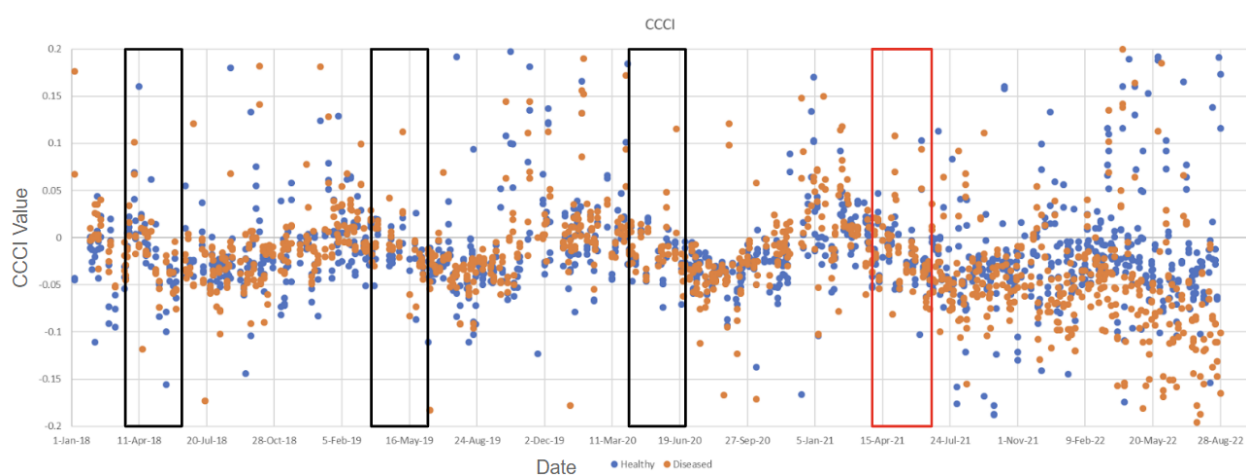


Figure 2: The spectral response plot for the CCCI spectral vegetation index for healthy (blue) and diseased (orange) trees. The trees are believed to have become infected in 2020. This plot highlights the difficulty of separating healthy from unhealthy trees. The boxes are when early stage infection detection should take place. The red box is when the infection is believed to have occurred.

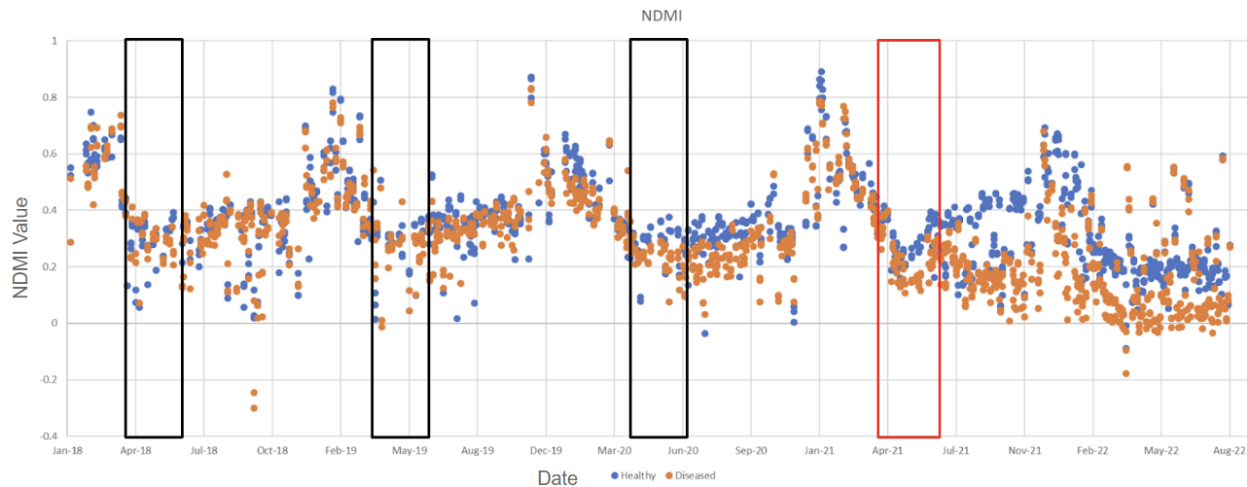


Figure 3: The spectral response plot for the NDMI spectral vegetation index for healthy (blue) and diseased (orange) trees. The trees are believed to have become infected in 2020. This plot highlights the difficulty of separating healthy from unhealthy trees. The boxes are when early stage infection detection should take place. The red box is when the infection is believed to have occurred.

The random forest methods also did not come with a definitive way to determine early stage bark beetle infestation. I compared points vs polygons as training, differenced spectral vegetation indices vs single time spectral vegetation indices, early may vs late May, and all spectral vegetation indices as inputs, vs selected ones. Early on, I recognized that polygons provided much more training data for the random forest model than points, so I opted to use polygons. After some early testing, I determined that the difference spectral vegetation index data as an input did not appear to be useful, so I only used the single temporal spectral vegetation index. This left a comparison for the selected inputs and the early vs late May input composite scenes. Table 3 has a list of the accuracies and F1 scores of the models. Though the validation accuracies are high, the F1 scores are low indicating a poor model. The random forest models which used all of the spectral vegetation indices as an input had a higher validation accuracy and F1 score than the selected spectral vegetation indices did. Also, for both selected and non-selected spectral vegetation indices, the late May image composite had a higher accuracy. The error matrices for the random forest models with the different inputs are found in Table 4 through Figure 8. In order to calculate the F1 score, which needs a binary value, I combined the noninfected trees into a single class to compare to the infected trees class.

Table 3: Accuracies of the random forest models.

Random Forest Inputs	Training Overall Accuracy	Validation Accuracy	F1 Score	Infected Trees Omission Error	Infected Trees Commission Error
Early May Data All Spectral Vegetation Indices	99.92%	93.95%	0.6373	21.01%	14.20%
Late May Data All Spectral Vegetation Indices	99.96%	97.16%	0.6581	15.38%	46.15%
Early May Data Selected Spectral Vegetation Indices	99.86%	93.68%	0.6016	19.79%	51.88%
Late May Data Selected Spectral Vegetation Indices	99.95%	94.02%	0.5185	38.46%	55.20%

Table 4: Validation error matrix for the early May Sentinel-2 data with all of the spectral vegetation indices as inputs.

	Snow	Shadow	Healthy Trees	Infected Trees	Bare Ground	Dead Trees
Snow	986	0	1	0	0	0
Shadow	0	72	0	0	0	0
Healthy Trees	5	0	851	15	0	0
Infected Trees	0	0	77	94	4	1
Bare Ground	0	0	0	6	11	0
Dead Trees	13	0	4	4	0	7

Table 5: Validation error matrix for the late May Sentinel-2 data with all of the spectral vegetation indices as inputs.

	Snow	Shadow	Healthy Trees	Infected Trees	Bare Ground	Cloud
Snow	626	0	0	0	1	15
Shadow	0	562	4	0	0	0
Healthy Trees	0	3	1101	14	1	0
Infected Trees	0	0	63	77	3	0
Bare Ground	2	0	0	0	114	0
Cloud	0	0	0	0	0	1148

Table 6: Validation error matrix for the early May Sentinel-2 data with the spectral vegetation indices that showed some separation during the early stage infection window as inputs.

	Snow	Shadow	Healthy Trees	Infected Trees	Bare Ground	Dead Trees
Snow	906	0	6	0	0	0
Shadow	0	59	0	1	0	0
Healthy Trees	9	0	859	10	0	0
Infected Trees	0	0	82	77	1	0
Bare Ground	0	0	0	2	19	0
Dead Trees	9	0	4	6	0	7

Table 7: Validation error matrix for the late May Sentinel-2 data with the spectral vegetation indices that showed some separation during the early stage infection window as inputs.

	Snow	Shadow	Healthy Trees	Infected Trees	Bare Ground	Cloud
Snow	580	1	0	0	0	38
Shadow	0	524	15	0	6	1
Healthy Trees	0	5	1029	32	2	0
Infected Trees	2	2	64	56	1	0
Bare Ground	1	2	15	3	111	0
Cloud	25	0	0	0	0	1080

Discussion

The thresholding approach did not appear to have any significant results since there was little separation between the healthy and diseased tree spectral vegetation index values during the early stage infection window. The random forest model appeared to be an accurate model because the validation accuracies are in the low to mid 90's. Though the accuracy may be high for all of the classes as a whole, the model is not accurate for the infected tree class, which is the most important class since it is the reason the model was created. The F1 scores ranged from 0.5185 to 0.6581 (Table 3). F1 scores range from 0 to 1 where 0 is an inaccurate model and a 1 is a perfect model. The F1 score balances precision and recall. Precision measures the percentage of predictions that have been labeled as positive that is correct. Recall measures the percentage of correctly classified true positives out of everything that should be labeled as positive. Not only is the F1 score low, but the infected tree class has very high omission and commission errors. The omission errors range from 15.38% to 38.46% with a mean of 23.66%. The commission errors range from 14.20% to 55.20% with a mean of 41.86%. High omission errors mean that the model under maps infected areas that should be mapped, and high commission errors mean that the model over maps areas that should be infected. The random forest models appear to do both, however, it appears to over map much more than is under maps. This over mapping effect can be seen clearly in Figure 4 - Figure 7. Figure 4 depicts images on the ground taken of dead bark beetle infested trees taken on July 14th, 2022. Figures 10 and 11 are planet images during the early stage detection window of the study site in both true color and NDVI for 2021 and

2022. The boxes in the upper right correspond to the images in Figure 4. Figure 7 is a Sentinel-2 composite image that is masked and the classified image. It is clear to see from the classified image that the infected trees (red) is greatly overrepresented in the final classification. The goal when creating the model is to help the local authorities to detect which trees are possibly experiencing early stage infection and for them to manually stop the spread. However, if the model over predicts the area infected, then the foresters would waste their limited time going to healthy trees. Plus, there are high omission errors, so some of the trees that they would go to may not even be infected.

This study had a few limitations that made the execution of the early stage bark beetle infestation detection challenging. The three challenges were the training data, validation data, and extreme slopes. In order to create an accurate machine learning model, a lot of training data is needed, and it needs to be of good quality. I created training data by manually labeling areas that had visible signs of grey/dead trees in 2022 but none in 2021. I used polygons for the final model, but polygons may suffer from spatial autocorrelation since the pixels in the polygon are next to each other. The tradeoff is to use points, but have fewer. A more robust study will use points from a bigger area in order to gain more data points but without the risk of spatial autocorrelation. I believe the labeled trees were attacked by bark beetles, but I do not know for certain if they were. So it is possible that the trees were dying from another cause. I would need ground validation data to know if they were attacked, and when. I had access to polygons that encircled areas that have been attacked by bark beetles from the local Avalanche and Torrent Control Agency, but it was uncertain when the trees in the polygons were attacked, and which trees in the polygons were infected. It appeared that the polygons were broadly drawn and had both infected and non-infected trees. Plus, trees that I marked as uninfected could have been infected but were still in the green phase. I did my best by looking at high resolution satellite imagery, but without highly detailed ground truth data, it is hard to make accurate training data.



Figure 4: Pictures from the ground of tree mortality on July 14th, 2022 (photo credit Chandler Ross).

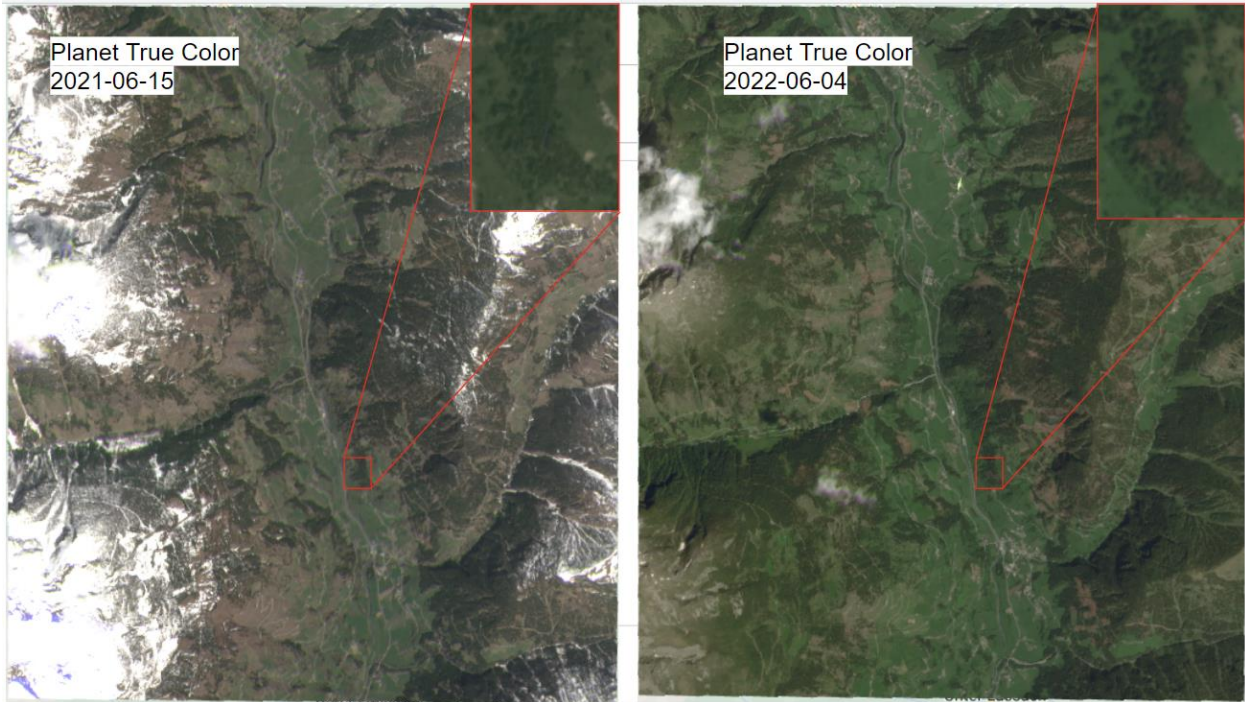


Figure 5: The left image shows a Planetscope true color image of the study site on June 15th, 2021. The right image is a Planetscope true color image of the study site on June 4th, 2022. The boxes in the upper right correspond to the images in Figure 4.

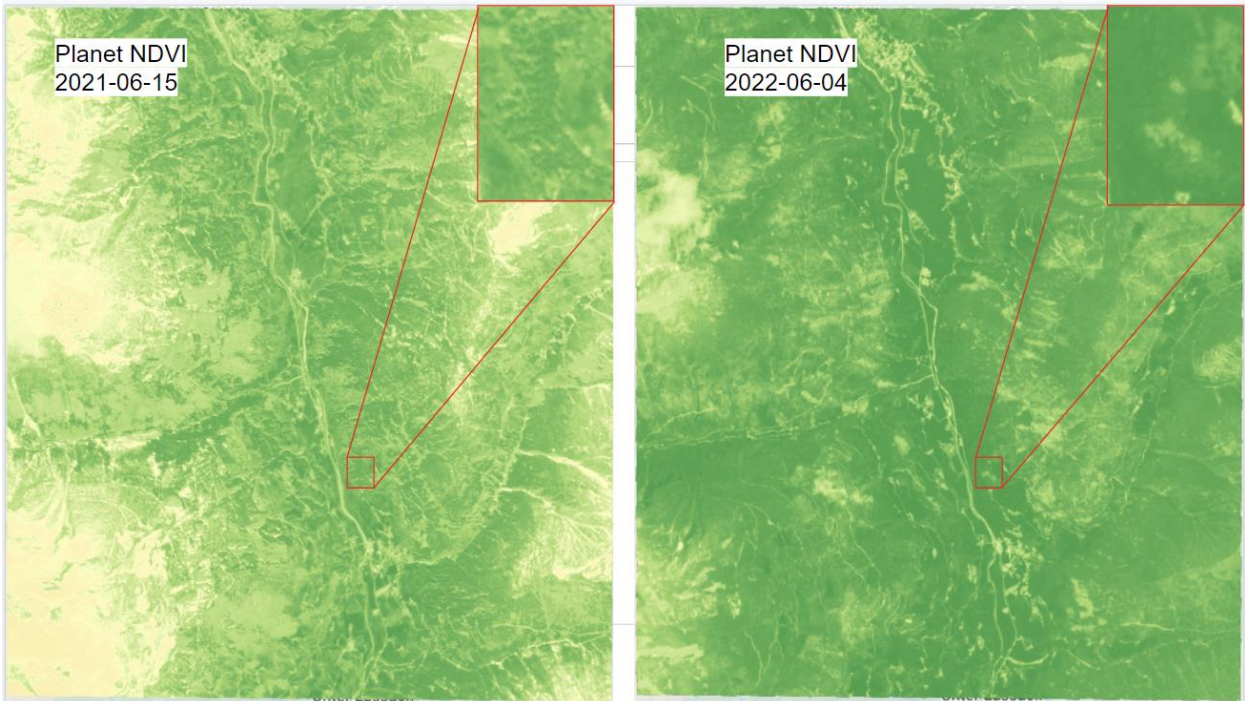


Figure 6: The left image shows a Planetscope NDVI image of the study site on June 15th, 2021. The right image is a Planetscope NDVI image of the study site on June 4th, 2022. The boxes in the upper right correspond to the images in Figure 4.

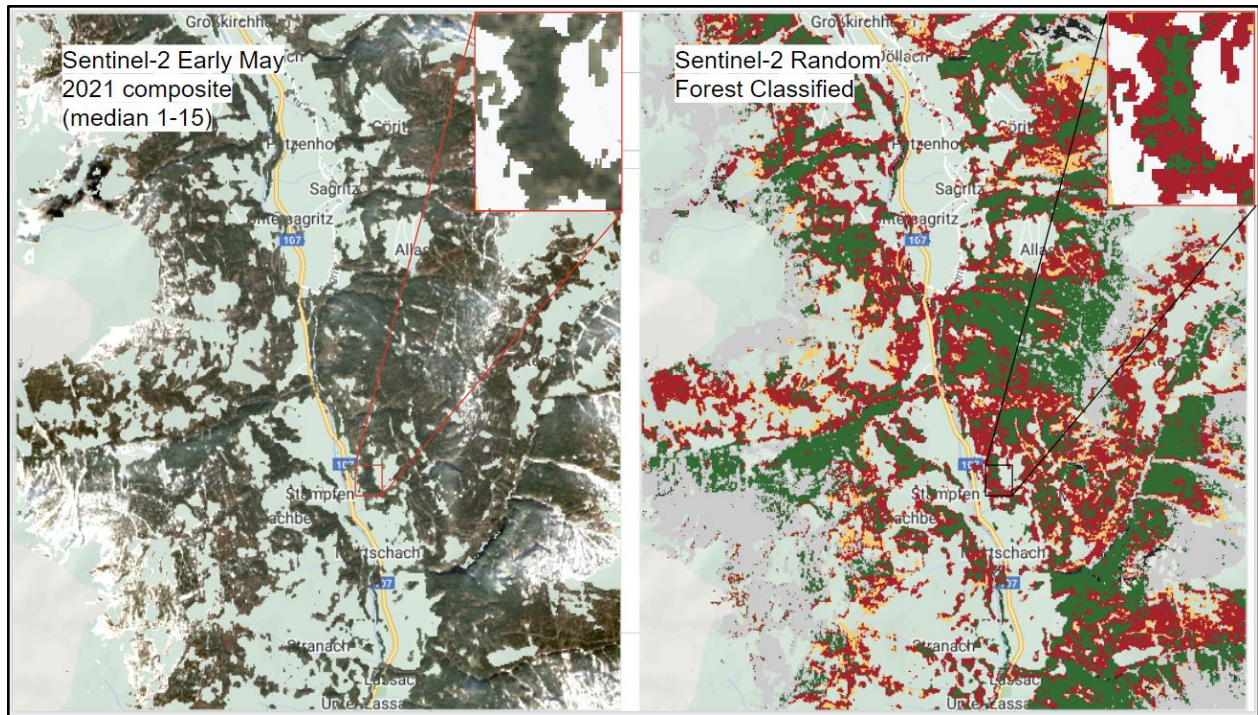


Figure 7: The image on the left is a masked Sentinel-2 composite image from May 1st to May 15th. The image on the right is a classified image from a random forest model. Green is healthy trees, red is predicted infected trees, black is shadow, yellow is bare ground, grey is snow, and brown is dead trees. The boxes in the upper right correspond to the images in Figure 4.

The last challenge is the extreme slopes of the study site. The study site was located in a valley with elevations from 909 m to 2,589 m above sea level. The steep slopes create issues for remote sensing since the ground is distorted in the images from the terrain. The terrain also caused issues with shadows, especially with the PlanetScope imagery. Since the Planet data was captured at different times, the shadows would change. Thus, the PlanetScope imagery was used for visual interpretation rather than for spectral analysis. Fortunately, the Sentinel-2 imagery is captured at the same time so it can be more easily compared.

Conclusion

After trying to find appropriate spectral vegetation index thresholds and running the random forest models, I was not able to create an accurate model to detect early stage bark beetle infestation for the Norway Spruce in the southern Austrian Alps. There was no significant deviation between the spectral responses between the healthy and infected trees during the detection window. The random forest predicted areas that were infected, but the omission errors were high and the commission errors were even higher. The most accurate model, which used late May composited data with all spectral vegetation indices as an input, had a validation accuracy of 97.16%, an F1 score of 0.6581, an omission error of 15.38%, and a commission error of 46.15%. However, the model with the lowest omission and commission errors, was the

early May data with all the spectral vegetation indices as an input, with a validation accuracy of 93.95%, F1 score of 0.6373, omission error of 21.01%, and a commission error of 14.20%. It is likely that the model did not do well because of a lack in quantity and quality of the training data. However, it is possible that the 10 m Sentinel-2 resolution was not high enough for early stage bark beetle detection. Further studies should be conducted to determine the cause of the misclassification.

Future Work

Though the random forest method in this paper did not work, it does not mean that it is completely useless. The random forest approach may still have potential. Future research should focus on creating more training data, and if possible using training data that has ground validation for when the trees have been infected by bark beetles. In this study, I compared different spectral vegetation indices and found that using all of them led to the most accurate results, however, I did not compare different input parameters. Google Earth Engine has six different input parameters: the number of trees, the number of variables per tree split, minimum leaf population size, a bag fraction size, and the number of the maximum number of nodes. By comparing different inputs for each, a more accurate result may be obtained.

Moving beyond a random forest, a more robust machine learning model, such as a convolutional neural network could be used to detect early stage bark beetle infestation. However, this method is not available in Google Earth Engine, so the Sentinel-2 data would need to be downloaded and stored, plus the model would have to be run in python which could be more costly and complex for the Avalanche and Torrent Control Agency. However, these drawbacks could be worth it if it leads to a more accurate classification.

An alternative method to machine learning would be a Continuous Change Detection Classification algorithm. This method is capable of detecting change with each new Sentinel-2 scene inputted into the model. This could be useful for determining a change in bark beetle infestation since there is only a small window where change is possible. However, it may be more useful to use the algorithm for detecting tree stress before the green stage attack window since stressed trees are more susceptible to being attacked, plus stress is easier to detect than early stage infection. Whichever method is used in the future, the focus should be on detecting tree stress from January to June, especially after a major storm event, since it is the stressed trees that pose the greatest risk.

References

- Bright, B. C., Hudak, A. T., Kennedy, R. E., & Meddens, A. J. H. (2014). Landsat Time Series and Lidar as Predictors of Live and Dead Basal Area Across Five Bark Beetle-Affected Forests. *IEEE Journal of Selected Topics in Applied Earth Observations and Remote Sensing*, 7(8), 3440–3452. <https://doi.org/10.1109/JSTARS.2014.2346955>
- Farr, T. G., Rosen, P. A., Caro, E., Crippen, R., Duren, R., Hensley, S., Kobrick, M., Paller, M., Rodriguez, E., Roth, L., Seal, D., Shaffer, S., Shimada, J., Umland, J., Werner, M., Oskin, M., Burbank, D., & Alsdorf, D. (2007). The Shuttle Radar Topography Mission. *Reviews of Geophysics*, 45(2), RG2004. <https://doi.org/10.1029/2005RG000183>
- Giannetti, F., Pecchi, M., Travaglini, D., Francini, S., D'Amico, G., Vangi, E., Coccozza, C., & Chirici, G. (2021). Estimating VAIA Windstorm Damaged Forest Area in Italy Using Time Series Sentinel-2 Imagery and Continuous Change Detection Algorithms. *Forests*, 12(6), 680. <https://doi.org/10.3390/f12060680>
- Grabska, E., Hawryło, P., & Socha, J. (2020). Continuous Detection of Small-Scale Changes in Scots Pine Dominated Stands Using Dense Sentinel-2 Time Series. *Remote Sensing*, 12(8), 1298. <https://doi.org/10.3390/rs12081298>
- Hollaus, M., & Vreugdenhil, M. (2019). Radar Satellite Imagery for Detecting Bark Beetle Outbreaks in Forests. *Current Forestry Reports*, 5(4), 240–250. <https://doi.org/10.1007/s40725-019-00098-z>
- Hu, T., Myers Toman, E., Chen, G., Shao, G., Zhou, Y., Li, Y., Zhao, K., & Feng, Y. (2021). Mapping fine-scale human disturbances in a working landscape with Landsat time series on Google Earth Engine. *ISPRS Journal of Photogrammetry and Remote Sensing*, 176, 250–261. <https://doi.org/10.1016/j.isprsjprs.2021.04.008>
- Huo, L., Persson, H. J., & Lindberg, E. (2021). Early detection of forest stress from European spruce bark beetle attack, and a new vegetation index: Normalized distance red & SWIR (NDRS). *Remote Sensing of Environment*, 255, 112240. <https://doi.org/10.1016/j.rse.2020.112240>
- Immitzer, M., & Atzberger, C. (2014). Frühzeitige Erkennung von Borkenkäferbefall an Fichten mittels WorldView-2 Satellitendaten. *Photogrammetrie - Fernerkundung - Geoinformation*, 2014(5), 351–367. <https://doi.org/10.1127/1432-8364/2014/0229>
- Kennedy, R. E., Yang, Z., & Cohen, W. B. (2010). Detecting trends in forest disturbance and recovery using yearly Landsat time series: 1. LandTrendr — Temporal segmentation algorithms. *Remote Sensing of Environment*, 114(12), 2897–2910. <https://doi.org/10.1016/j.rse.2010.07.008>
- Klouček, T., Komárek, J., Surový, P., Hrach, K., Janata, P., & Vašíček, B. (2019). The Use of UAV Mounted Sensors for Precise Detection of Bark Beetle Infestation. *Remote Sensing*, 11(13), 1561. <https://doi.org/10.3390/rs11131561>
- Lausch, A., Heurich, M., Gordalla, D., Dobner, H.-J., Gwilym-Margianto, S., & Salbach, C. (2013). Forecasting potential bark beetle outbreaks based on spruce forest vitality using

- hyperspectral remote-sensing techniques at different scales. *Forest Ecology and Management*, 308, 76–89. <https://doi.org/10.1016/j.foreco.2013.07.043>
- Masiliūnas, D., Tsendbazar, N.-E., Herold, M., & Verbesselt, J. (2021). BFAST Lite: A Lightweight Break Detection Method for Time Series Analysis. *Remote Sensing*, 13(16), 3308. <https://doi.org/10.3390/rs13163308>
- Oeser, J., Pflugmacher, D., Senf, C., Heurich, M., & Hostert, P. (2017). Using Intra-Annual Landsat Time Series for Attributing Forest Disturbance Agents in Central Europe. *Forests*, 8(7), 251. <https://doi.org/10.3390/f8070251>
- Ortiz, S., Breidenbach, J., & Kändler, G. (2013). Early Detection of Bark Beetle Green Attack Using TerraSAR-X and RapidEye Data. *Remote Sensing*, 5(4), 1912–1931. <https://doi.org/10.3390/rs5041912>
- Senf, C., Pflugmacher, D., Wulder, M. A., & Hostert, P. (2015). Characterizing spectral –temporal patterns of defoliator and bark beetle disturbances using Landsat time series. *Remote Sensing of Environment*, 170, 166–177. <https://doi.org/10.1016/j.rse.2015.09.019>
- Verbesselt, J., Hyndman, R., Newnham, G., & Culvenor, D. (2010). Detecting trend and seasonal changes in satellite image time series. *Remote Sensing of Environment*, 114(1), 106–115. <https://doi.org/10.1016/j.rse.2009.08.014>
- Wermelinger, B. (2004). Ecology and management of the spruce bark beetle *Ips typographus*—A review of recent research. *Forest Ecology and Management*, 202(1–3), 67–82. <https://doi.org/10.1016/j.foreco.2004.07.018>
- Ye, S., Rogan, J., Zhu, Z., Hawbaker, T. J., Hart, S. J., Andrus, R. A., Meddens, A. J. H., Hicke, J. A., Eastman, J. R., & Kulakowski, D. (2021). Detecting subtle change from dense Landsat time series: Case studies of mountain pine beetle and spruce beetle disturbance. *Remote Sensing of Environment*, 263, 112560. <https://doi.org/10.1016/j.rse.2021.112560>
- Zanaga, D., Van De Kerchove, R., De Keersmaecker, W., Souverijns, N., Brockmann, C., Quast, R., Wevers, J., Grosu, A., Paccini, A., Vergnaud, S., Cartus, O., Santoro, M., Fritz, S., Georgieva, I., Lesiv, M., Carter, S., Herold, M., Li, Linlin, Tsendbazar, N.E., Ramoino, F., Arino, O., 2021. ESA WorldCover 10 m 2020 v100. ([doi:10.5281/zenodo.5571936](https://doi.org/10.5281/zenodo.5571936))
- Zhao, K., Wulder, M. A., Hu, T., Bright, R., Wu, Q., Qin, H., Li, Y., Toman, E., Mallick, B., Zhang, X., & Brown, M. (2019). Detecting change-point, trend, and seasonality in satellite time series data to track abrupt changes and nonlinear dynamics: A Bayesian ensemble algorithm. *Remote Sensing of Environment*, 232, 111181. <https://doi.org/10.1016/j.rse.2019.04.034>
- Zhu, Z., & Woodcock, C. E. (2014). Continuous change detection and classification of land cover using all available Landsat data. *Remote Sensing of Environment*, 144, 152–171. <https://doi.org/10.1016/j.rse.2014.01.011>
- Zhu, Z., Woodcock, C. E., & Olofsson, P. (2012). Continuous monitoring of forest disturbance using all available Landsat imagery. *Remote Sensing of Environment*, 122, 75–91. <https://doi.org/10.1016/j.rse.2011.10.030>